Imaging Odor-Induced Calcium Transients in Single Olfactory Cilia: Specificity of Activation and Role in Transduction

Trese Leinders-Zufall,[1] Charles A. Greer,[2,3] Gordon M. Shepherd,[2] and Frank Zufall[1]

[1]Department of Anatomy and Neurobiology, University of Maryland, Baltimore, Maryland 21201, and [2]Section of Neurobiology and [3]Department of Neurosurgery, Yale University School of Medicine, New Haven, Connecticut 06510

The possibility that odor stimuli trigger distinct Ca^{2+} elevations within the cilia of vertebrate olfactory receptor neurons (ORNs) is a widely proposed concept. However, because of the small size of the olfactory cilia, the existence and properties of such Ca^{2+} elevations and their role in odor transduction are still unknown. We investigate odor-induced Ca^{2+} changes in individual olfactory cilia from salamander using the Ca^{2+} indicator dye fluo-3 in combination with laser scanning confocal microscopy. Single brief applications of odor ligand produce highly localized Ca^{2+} elevations in individual cilia lasting for several seconds. These Ca^{2+} signals originate in the cilia and depend entirely on Ca^{2+} entry through ciliary cyclic nucleotide-gated ion channels. The odor specificity of the Ca^{2+} rises implies a receptor-operated mechanism underlying odor detection. Each of the cilia on a receptor neuron functions as an independent biochemical compartment that can detect odorants and produce a Ca^{2+} transient with remarkably uniform properties in terms of kinetics and odor specificity. The rate of recovery of the odor-induced Ca^{2+} transients matches recovery from a short-term form of odor adaptation. Application of the membrane-permeant intracellular Ca^{2+} chelator BAPTA AM eliminates this odor adaptation. The results indicate that an olfactory cilium serves as a basic functional unit at the input level of the olfactory system, controlling both the specificity and sensitivity of odor detection.

Key words: olfactory receptor neurons; cilia; confocal microscopy; imaging; cAMP; calcium signaling; cyclic nucleotide-gated channels; salamander; sensory adaptation; G-protein-coupled second messenger pathway, BAPTA AM

The initial transduction steps leading to olfactory perception occur in olfactory sensory neurons where odor ligands are believed to bind to specific receptor proteins (Buck and Axel, 1991; Zhao et al., 1998). This initiates a second messenger cascade causing rapid formation of cAMP (Pace et al., 1985; Sklar et al., 1986; Breer et al., 1990; Reed, 1992; Belluscio et al., 1998) followed by the opening of cyclic nucleotide-gated (CNG) cation channels (Nakamura and Gold, 1987; Kurahashi, 1990; Dhallan et al., 1990; Firestein et al., 1991a,b; Brunet et al., 1996).

These initial events are believed to take place in the cilia of the olfactory sensory neurons. Electrophysiological studies have provided evidence for this at the level of the bundle of cilia of a single sensory neuron (Firestein et al., 1990; Lowe and Gold, 1991, 1993a). However, the small diameters (0.2–0.3 μm) have thus far been an impediment to obtaining spatial and temporal resolution of transduction events within individual cilia. This is necessary for addressing several critical aspects of the transduction mechanism: the initiation of the odor-induced response; variations or equivalence of the odor response in the different cilia of a single cell; the possibility of compartmentation within a single cilium; and testing for propagation of transduction-associated biochemical events through the cilia and into the dendritic knob and dendrite of the sensory neuron. Analysis of similar questions in the stereocilia of mechanosensory hair cells has used dye indicators to image ion movements in individual cilia (Denk et al., 1995; Lumpkin and Hudspeth, 1995).

The olfactory CNG channels have been shown to have a nonspecific cation permeability, including a significant Ca^{2+} component (Nakamura and Gold, 1987; Zufall et al., 1991a; Frings et al., 1995; Zagotta and Siegelbaum, 1996; Leinders-Zufall et al., 1997a). The Ca^{2+} elevations resulting from CNG channel activation are believed to be important for odor amplification and adaptation, thus providing the basis for sensitivity regulation of odor detection (Kurahashi and Shibuya, 1990; Zufall et al., 1991b; Lowe and Gold, 1993b; Kurahashi and Menini, 1997). Earlier studies using Ca^{2+} indicator dyes have demonstrated whole-cell Ca^{2+} elevations in response to odor stimulation or pharmacological treatments (Lischka and Schild, 1993; Restrepo et al., 1993; Nakamura et al., 1994; Sato et al., 1994; Tareilus et al., 1995; Bozza and Kauer, 1997; Morales et al., 1997), but these studies have not addressed Ca^{2+} signals in the olfactory cilia. Recently we have extended this approach to image optically Ca^{2+} changes in individual salamander olfactory cilia resulting from activation of CNG channels after manipulation of the intracellular cyclic nucleotide concentration (Leinders-Zufall et al., 1997a). With this assay, we are now able to detect odor-stimulated Ca^{2+} signals in single olfactory cilia with submicrometer spatial resolution and millisecond temporal resolution. We show that odor-induced ciliary Ca^{2+} transients are similar to those produced by CNG channel activation; we map the odor sensitivity of individual olfactory cilia and characterize the func-

Received March 23, 1998; revised May 6, 1998; accepted May 11, 1998.

This work was supported in part by National Institute of Neurological Diseases and Stroke (NINDS) Grant RO1 NS37748 to F.Z.; National Institute on Deafness and Other Communication Disorders (NIDCD) Grants R29 DC003773 to T.L.-Z., RO1 DC 00086 to G.M.S., and RO1 DC 00210 to C.A.G.; NINDS Grant P50 NS10174 to C.A.G.; and NIDCD, NASA, and National Institute of Mental Health under the Human Brain Project Grant RO1 MH52550 to G.M.S. We thank Dr. Mark N. Rand for help during an early phase of this project.

Correspondence should be addressed to Dr. Frank Zufall, Department of Anatomy and Neurobiology, University of Maryland, 685 West Baltimore Street, Baltimore, MD 21201.

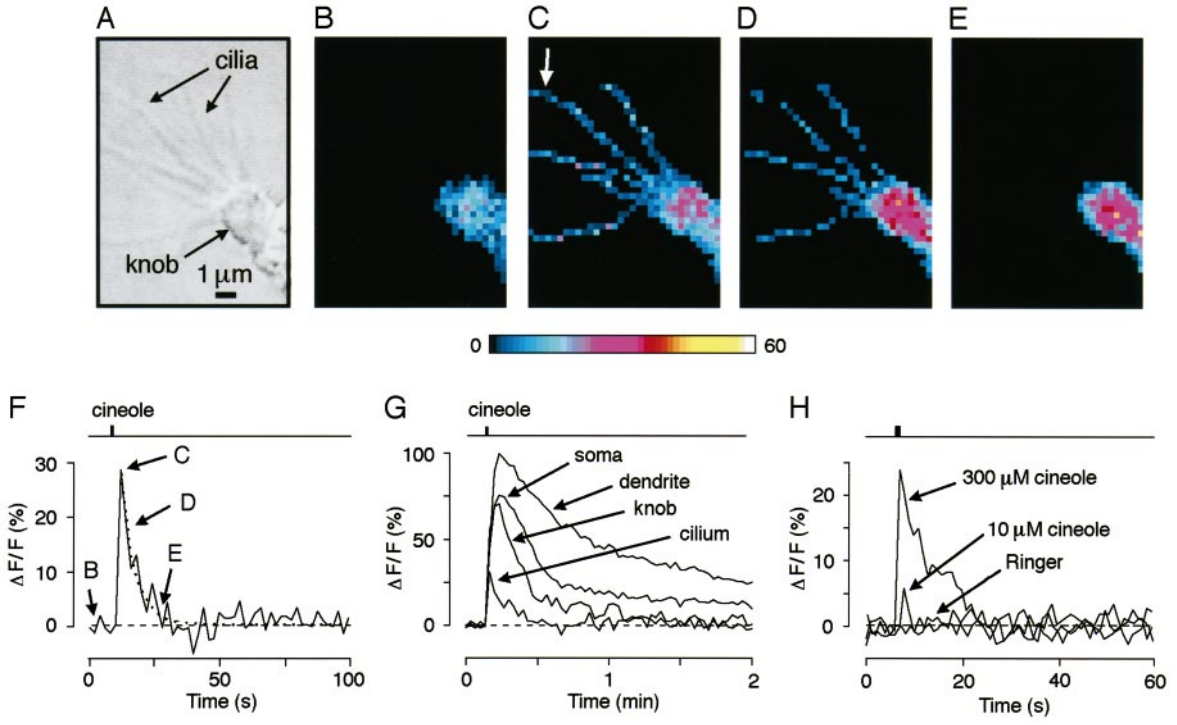

Figure 1. Optical imaging reveals transient Ca^{2+} elevations in individual olfactory cilia after the application of a single pulse (1 sec) of odor ligand (cineole, 300 μM). *A*, Phase-contrast image of a salamander olfactory receptor neuron (ORN) showing several cilia emanating from an olfactory knob. *B–E*, Fluorescence images (pseudocolor scale) taken at rest in the absence of odor ligand (*B*), near peak fluorescence 2 sec after triggering the odor stimulus (*C*), and 4 sec (*D*) and 16 sec (*E*) after stimulation. At rest, the knob and part of the dendrite are visible, but resting Ca^{2+} fluorescence in the cilia is below the resolution limit. Odor stimulation leads to transient Ca^{2+} accumulation in the cilia. Note in *E* that the ciliary signal has declined back to baseline, whereas Ca^{2+} accumulation remains high in the dendritic knob. Individual frames recorded at 0.5 Hz. *F*, Time course of an odor-induced ciliary Ca^{2+} transient (taken from the cilium labeled by the *white arrow*). The decay time course was fitted with a monoexponential function (*dotted line*) yielding a time constant of 5.3 sec. Timing of the stimulus is indicated in the trace above the Ca^{2+} response. Labeling indicates the time points for which individual frames were printed. *G*, Comparison of the time course of odor-induced Ca^{2+} changes (single stimulus) in various ORN compartments. Data are from the same neuron as shown in *A–F*. *H*, Time course and peak amplitude of the ciliary signal depends on odorant concentration (different experiment). Odor-free Ringer's solution is unable to elicit Ca^{2+} transients.

tion of the odor-induced Ca^{2+} changes in relation to sensory adaptation and odor sensitivity regulation.

Preliminary results have been published in abstract form (Leinders-Zufall et al., 1997b).

MATERIALS AND METHODS

Preparation and solutions. The methods used in this study followed closely protocols devised previously (Leinders-Zufall et al., 1997a). Briefly, olfactory receptor neurons (ORNs) were acutely dissociated from the nasal epithelium of adult land-phase tiger salamanders (*Ambystoma tigrinum*) without the use of enzymes. To avoid movement artifacts suspended cells were placed in a laminar flow chamber on glass coverslips that had been previously coated with 0.1% laminin and 0.01% poly-L-lysine to immobilize the neurons and their normally motile cilia on the substrate. Only those cilia that did not change their position during the course of an experiment were included in the analysis. ORNs were continuously superfused with physiological Ringer's solution containing (in mM): NaCl 115, KCl 2.5, $CaCl_2$ 1.0, $MgCl_2$ 1.5, HEPES 4.5, and Na HEPES 4.5, pH 7.6, adjusted to 240 mOsm. To avoid a contribution to the measured Ca^{2+} signals from regenerative action potential discharges, 4 μM tetrodotoxin (TTX) was added to this solution in all experiments. All measurements were performed at room temperature.

Calcium imaging, calibration, and data analysis. Imaging techniques were essentially as described (Leinders-Zufall et al., 1997a). ORNs were loaded with the Ca^{2+} indicator fluo-3 AM (18 μM; Molecular Probes, Eugene, OR). A laser scanning confocal system (MRC-600; Bio-Rad, Hercules, CA) attached to an Olympus IMT-2 inverted microscope was used to visualize Ca^{2+}-mediated fluorescence changes. A 60×, 1.4 numeric aperture objective (Nikon) was used; images were additionally magnified 3–4× using the confocal's electronic zoom setting. Time-series images were made by collecting 64 × 64 pixel fluorescence images at a rate of 0.5, 1 or 3 Hz. For higher spatial resolution required in some experiments, four individual frames (768 × 512 pixels/frame) were averaged together, using the Kalman filter function of the confocal system. To obtain images at high temporal resolution, we used the line scan mode of the confocal system (11.7 msec/line, 512 lines). Data are presented in arbitrary fluorescence units or as relative changes in fluorescence intensity normalized to baseline fluorescence ($\Delta F/F$). Calibration of fluorescence signals was performed by the use of Ca^{2+} ionophore and heavy metal chelation as detailed in Kao et al. (1989) and Leinders-Zufall et al. (1997a).

For off-line analysis, eight-bit confocal image files were transferred to a Macintosh Quadra 800 microcomputer and analyzed with NIH Image 1.59 software. Additional data analyses, calculations, and fitting procedures were performed using Igor Pro software (WaveMetrics, Lake Oswego, OR). Data are expressed as mean ± SD. To generate odor response profiles (see Figs. 2, 7) we calculated the area under each Ca^{2+} response using the trapezoidal integration function of the Igor Pro software. Areas were normalized to the maximum response obtained from stimulation with the phosphodiesterase inhibitor IBMX. Each value was plotted as a circle with its area equivalent to the measured integral of the corresponding Ca^{2+} response.

Odor stimulation. The following odor ligands were used in this study: acetophenone (1-phenylethanone; Sigma, St. Louis, MO), *n*-amyl acetate (Sigma), isoamyl acetate (acetic acid 3-methylbutyl ester; Sigma), cineole (eucalyptol, 1,3,3-trimethyl-2-oxabicyclo[2,2,2]-octane; Sigma), citralva (3,7-dimethyl-2,6-octadienenitrile; Aldrich, Milwaukee, WI), and ethyl butyrate (ethyl *n*-butyrate; Aldrich). The purity grade of all odor compounds was 99% except for citralva, which had a purity grade of 97%. Odor solutions were prepared as previously described (Leinders-Zufall et al., 1996). Odor stimuli were ejected from multibarrel glass pipettes

that were placed within 5–10 μm from the cilia. Stimulus pipettes were located downstream from the cells to avoid prestimulation. Under these conditions, the solution switching time was 30–40 msec as measured by the electrical response to elevated K^+ solutions.

Electrophysiology. Odor-stimulated membrane currents were recorded under voltage clamp (holding potential, −60 mV) by applying the perforated-patch technique with amphotericin B (Leinders-Zufall et al., 1995; 1996). This approach ensures the least possible disturbance of the internal milieu of the neurons and prevents artificial Ca^{2+}-buffering from influencing the results. Current recording, stimulation sequences, data acquisition, and on-line analysis were controlled by an EPC-9 patch-clamp amplifier in combination with Pulse software (HEKA Electronic) and a Macintosh computer. Currents were filtered at 300 Hz (−3 dB, eight-pole low-pass Bessel) and digitally sampled at 5 msec/point. The indifferent electrode consisted of an Ag–AgCl wire connected to the bath solution via an agar bridge. All data reported here have been corrected for junction potentials.

Our basic paradigm to study short-term odor adaptation was to elicit paired pulses of the same intensity and duration (100 msec) while varying the interpulse interval from 2 to 14 sec (Kurahashi and Shibuya, 1990; Kurahashi and Menini, 1997). The interval between two paired pulses was 40 sec. The cell-permeant intracellular Ca^{2+} chelator 1,2-bis-(2-amino-phenoxy)ethane-*N,N,N′,N′*-tetra-acetic acid AM (BAPTA AM; Molecular Probes) was dissolved in a solution of DMSO and 6% Pluronic F-127 (Molecular Probes) that was then added to normal Ringer's solution, sonicated, and added to the experimental chamber to give a final concentration of 100 μM BAPTA AM, 0.18% DMSO, and 0.012% Pluronic F-127.

RESULTS

Detection of odor-induced ciliary calcium transients

To investigate odor-induced Ca^{2+} changes in individual olfactory cilia, salamander ORNs were freshly isolated from the nasal epithelium, immobilized on the substrate, and loaded with the Ca^{2+} indicator dye fluo-3 AM. In this preparation, individual cilia (with a diameter of ~0.3 μm) can be visualized using confocal laser scanning microscopy, and odor molecules can be applied to single cilia by micropulse stimulation (Leinders-Zufall et al., 1997a). The results described in this report are based on a population of 176 ORNs.

In the presence of TTX (4 μM), we observed odor-induced Ca^{2+} transients in individual cilia after a single 1 sec pulse of odor ligand (cineole, 300 μM) (Fig. 1*A–F*). These transients rose to a peak within 2 sec after stimulus triggering and then decayed on an exponential time course with a time constant of 5.5 ± 2.2 sec (SD, 12 ORNs, 48 cilia) (Fig. 1*F*). The relatively small SD of the decay time constant indicates the robustness and consistency of this response, at least at the odor concentration used here. The odor pulse also caused Ca^{2+} increases in other compartments of the ORN, including the dendritic knob, dendrite, and soma, but these Ca^{2+} changes showed very different dynamics compared with those in the cilia and were sustained for much longer periods (Fig. 1*G*). The temporal behavior of these differential Ca^{2+} responses in the various neuronal compartments resembled closely the changes observed after manipulation of the intracellular cyclic nucleotide concentration using brief pulses of the phosphodiesterase inhibitor 3-isobutyl-1-methylxanthine (IBMX; Leinders-Zufall et al., 1997a), suggesting that they could arise from Ca^{2+} entry through CNG channels activated by the well known cAMP second messenger system of these cells (for review, see Zufall et al., 1994). The peak amplitude of the ciliary Ca^{2+} transients was highly dependent on the odor concentration. In the example shown in Figure 1*H*, a pulse of 300 μM cineole caused a relative change in the peak fluorescence ($\Delta F/F$) of ~24%, whereas 10 μM cineole led to a much smaller (and shorter) change of ~6%. Odor-free Ringer's solution had no effect (Fig. 1*H*). Similar results were obtained in six ORNs. These data are consistent with the steep dose–response behavior of odor-induced membrane currents in these cells (Firestein et al., 1993; Leinders-Zufall et al., 1996).

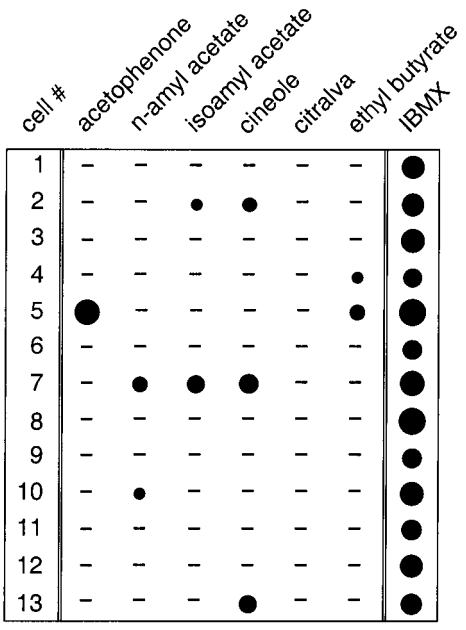

Figure 2. Matrix illustrating the odor specificity of ciliary Ca^{2+} transients. The effects of six different odor ligands (acetophenone, *n*-amyl acetate, isoamyl acetate, cineole, citralva, and ethyl butyrate; all at 300 μM) and their capacity to trigger ciliary Ca^{2+} transients are tested in 13 individual ORNs. Each cell was also stimulated with the phosphodiesterase inhibitor IBMX (300 μM) to prove that it was alive and contained an intact cyclic nucleotide second messenger system. Size of circles corresponds to the magnitude of Ca^{2+} responses calculated as area under each curve (see Materials and Methods). Values are expressed as a percentage of the maximum IBMX response (cell 5, 100%). The smallest circle (cell *10*, *n*-amyl acetate) corresponds to 18%. A response from a given cell represents the mean of two to four ciliary Ca^{2+} transients. The *minus sign* means that no detectable signals were present in response to that odor ligand.

It should be noted that the imaging of a single cilium showed variations in distribution of fluorescence intensity at the single pixel level. Thus, in Figure 1, *C* and *D*, the Ca^{2+} signals appear as punctae or beads along the lengths of the cilia. Further analysis of these "hot spots" showed that they are unlikely to be random events (data not shown). It is therefore possible that they reflect inhomogeneities in the localization of CNG channels or of other components of the sensory transduction machinery. We will discuss these possibilities later.

Olfactory cilia control the specificity of odor detection

If the Ca^{2+} transients are a direct consequence of the olfactory signaling pathway and reflect odor receptor activation, then they should exhibit odor specificity and depend on the nature of the odor ligand; this odor specificity should vary substantially between individual ORNs. Two lines of evidence demonstrate that this was the case. First, only a subset of the neurons (41 of 137 ORNs; 29.9%) generated detectable Ca^{2+} transients in response to cineole, even when we used relatively high doses of the odor ligand (300 μM) that are known to saturate sensory membrane currents (Firestein et al., 1993; Leinders-Zufall et al., 1996). This result indicates that the Ca^{2+} transients cannot simply be explained by nonspecific actions of the odor ligand at the ciliary membrane. Second, we explored systematically the effects of six

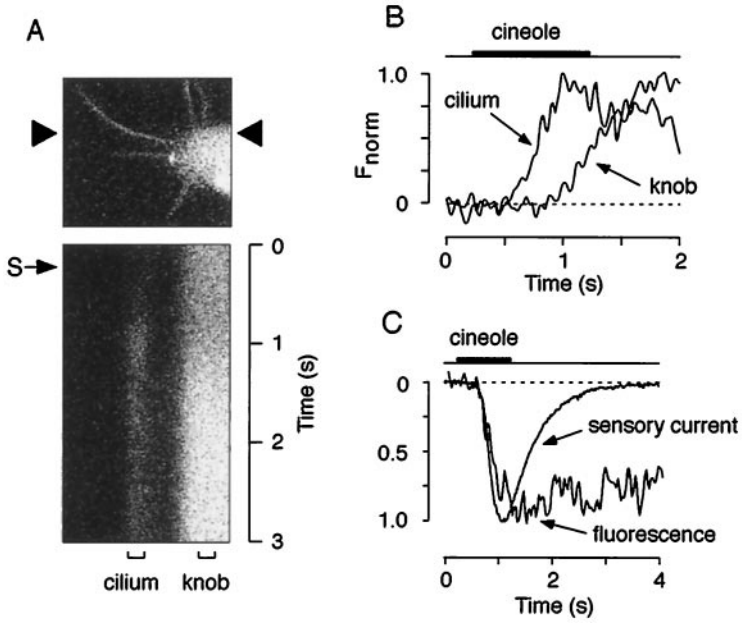

Figure 3. Events underlying odor detection are initiated in the olfactory cilia. *A*, Fluorescence image (*top*, *gray scale*) and high temporal resolution line scan (*bottom*) of a ciliary array and part of the knob of an ORN. The position of the line that was scanned successively every 11.7 msec is indicated by *arrowheads*. A single 1 sec pulse of cineole (*S*, *small arrow*; 300 μM) produced a transient fluorescence increase after a delay of 273 msec that reached its peak 772 msec after triggering of the odor pulse and then decayed back to baseline level. Note that the fluorescence increase in the knob occurred later than in the cilium and was less transient. *B*, Plot of the time course of the Ca^{2+} signals (normalized responses) of the areas indicated by the *brackets* labeled with *cilium* and *knob* in *A*. There was a pronounced delay of 351 msec between the Ca^{2+} rise in the cilium and the knob. *C*, Comparison of the kinetic properties of odor-induced membrane currents with ciliary Ca^{2+} transients. Representative waveforms of the sensory current (average current from 3 individual ORNs; see Materials and Methods for details) produced by a 1 sec pulse of cineole (300 μM) and ciliary Ca^{2+} transients generated by the same stimulus (average response of 4 cilia from different ORNs) were superimposed (normalized responses) (compare Table 1).

different odor ligands and tested their capacity to trigger Ca^{2+} transients (Fig. 2). For this experiment we used acetophenone, *n*-amyl acetate, isoamyl acetate, cineole, citralva, and ethyl butyrate (all at 300 μM). After an experimental series, each cell was stimulated with the phosphodiesterase inhibitor IBMX (300 μM) to prove that it was alive and contained an intact cyclic nucleotide second messenger system. Of 13 ORNs tested in this way, each one responded with a robust ciliary Ca^{2+} transient to IBMX as described previously (Leinders-Zufall et al., 1997a) (Fig. 2). In contrast, the probability of eliciting odor-induced Ca^{2+} transients was much lower: seven cells showed no odor responses, three cells responded only to one ligand, two cells responded to two, and one cell responded to three ligands (Fig. 2). In no case did we detect an identical response spectrum. Interestingly, in two cases the cilia were able to discriminate between the isomers *n*-amyl acetate and isoamyl acetate (see cells *2* and *10*, Fig. 2).

These results are consistent with the discriminative properties of salamander ORNs as revealed by analyzing electrical membrane currents at the whole-cell level (Firestein et al., 1993). Taken together, our data rule out that the Ca^{2+} transients were caused by nonspecific actions of odor ligand in the ciliary membrane but suggest that they result from a relatively specific receptor-operated mechanism. Thus, the Ca^{2+} transients likely reflect interactions of odor molecules with olfactory receptor proteins.

Kinetic and pharmacological analysis of odor-induced ciliary calcium transients

What is the precise mechanism for the odor-induced ciliary Ca^{2+} elevations? In view of the substantial Ca^{2+} permeability of the CNG channels, it seemed reasonable to hypothesize that the signals resulted from Ca^{2+} entry through CNG channels after activation of the odor-stimulated cAMP pathway of these neurons. To test this notion further, several additional types of experiments were performed.

If the transients are a consequence of CNG channel activation, then their kinetic properties should be consistent with those of CNG channel-mediated sensory currents. The results depicted in Figure 3 and Table 1 demonstrate that this was the case. ORNs

Table 1. Comparison of the kinetic properties of odor-stimulated membrane currents and ciliary Ca^{2+} transients

	Odor-induced membrane current	Odor-induced ciliary Ca^{2+} transient
Delay (msec)	296 ± 30	358 ± 86
	(n = 3)	(n = 4)
Rise time (msec)	589 ± 60	912 ± 344
	(n = 3)	(n = 4)
Half-recovery time (msec)	702 ± 163	4153 ± 1934
	(n = 3)	(n = 48)

For recording of membrane currents, ORNs were voltage-clamped to −60 mV and stimulated with a 1 sec pulse of cineole (300 μM). The same stimulus was used for eliciting Ca^{2+} responses. Ca^{2+} responses were obtained using the line-scan method as shown in Figure 3. The delay was measured from triggering the stimulus to the point at which the response exceeded twice the SD of the mean of the baseline noise. Rise time was measured from this point to the peak of the response. Half-recovery time was measured from the peak of the response to 50% recovery.

were imaged at high temporal resolution using time-resolved line scans (11.7 msec/line, 512 lines) (Fig. 3*A*). This approach revealed that the earliest odor-induced Ca^{2+} changes occurred in the cilia, followed by Ca^{2+} increases in the dendritic knob (Fig. 3*B*). There was a pronounced delay of 265 ± 94 msec (n = 4 ORNs) between the Ca^{2+} elevation in a given cilium and the knob (Fig. 3*B*). Together with the results of Figure 1*G*, the data demonstrate that events underlying odor detection are initiated in the cilia. The delay between the signal onset in cilia and knob is especially notable, because it means that during that time there is no evidence for back spread of Ca^{2+} from the dendritic knob. This indicates that each cilium can detect the presence of odor ligand and can function as a Ca^{2+}-signaling unit independent of each other and of events in the dendritic knob. Comparison of the kinetic properties of the Ca^{2+} transients with cineole-induced membrane currents obtained under voltage clamp using the perforated patch-clamp method (Fig. 3*C*, Table 1) revealed that both the initial delay and onset time course of the ciliary Ca^{2+} transients were fully consistent with Ca^{2+} entry through CNG channel activation. In contrast, there was very little temporal correlation between the deactivation phase of the ciliary Ca^{2+} transients

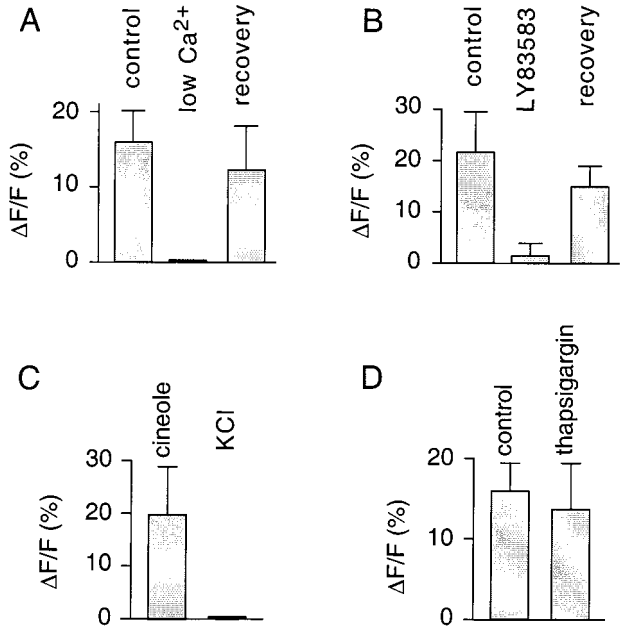

Figure 4. Pharmacological properties of odor-induced ciliary Ca^{2+} transients (triggered by 300 μM cineole). *A*, Plot of Ca^{2+} peak responses (3 ORNs, 8 cilia) under control conditions, with lowered Ca^{2+} (0.6 μM) in the external bath solution, and after restoration of normal Ca^{2+} levels. *B*, Ca^{2+} peak responses (3 ORNs, 9 cilia) under control conditions, in the presence of LY83583 (50 μM), and after washout of the drug. *C*, Comparison of the Ca^{2+} response resulting from a pulse of cineole or KCl (120 mM) (3 ORNs). Note that KCl is unable to elicit any detectable Ca^{2+} changes in the cilia. *D*, Comparison of Ca^{2+} peak responses before and after treatment of the cells with the Ca^{2+}–ATPase inhibitor thapsigargin (200 nM) (3 ORNs, 8 cilia). There was no significant difference, indicating that Ca^{2+} stores were not required for the generation of ciliary Ca^{2+} transients.

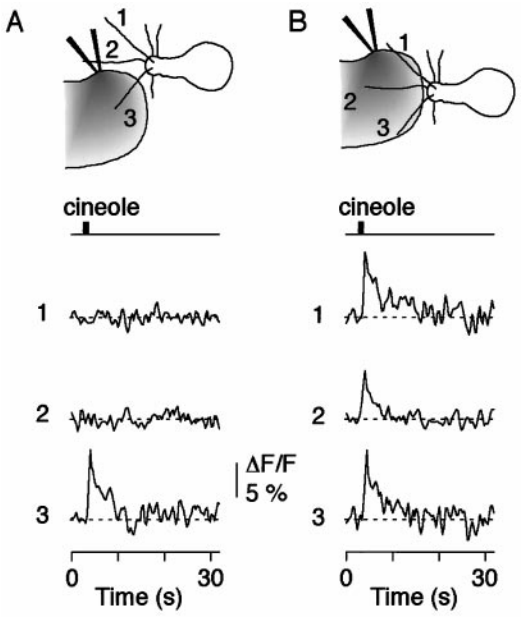

Figure 5. Olfactory cilia as individual neuronal compartments for odor detection. *A*, Application of a spatially restricted odor pulse (cineole, 100 μM) to cilium 3 produced a Ca^{2+} transient in that cilium. Note that there was no detectable response in the two remaining cilia. *B*, That all cilia were responsive to the odor pulse was shown by directing the stimulus at all three cilia and analyzing the resulting Ca^{2+} transients.

and the sensory currents, suggesting that the mechanisms governing the clearance from the Ca^{2+} load are likely to be independent from CNG channel opening and closing (Table 1).

As a further test of the origin of the measured fluorescence signals, the external Ca^{2+} concentration was lowered to 0.6 μM (Fig. 4*A*). This treatment abolished signals in a reversible manner ($n = 3$ ORNs), demonstrating that Ca^{2+} entry was required (Fig. 4*A*). The odor-induced transients were also strongly diminished by applying LY83583 (50 μM) (4.9 ± 7.8% of control; $n = 3$ ORNs; Fig. 4*B*), a potent reversible blocker of Ca^{2+} fluxes through olfactory CNG channels (Leinders-Zufall and Zufall, 1995; Leinders-Zufall et al., 1997a). Given the absence of voltage-gated Ca^{2+} channels in olfactory cilia (Fig. 4*C*) (also see Leinders-Zufall et al., 1997a) and that irreversible depletion of Ca^{2+} stores with the Ca^{2+}–ATPase inhibitor thapsigargin (200 nM) had no significant effect on the ability of the neurons to produce odor-induced Ca^{2+} responses in the cilia (Fig. 4*D*) (also see Zufall et al., 1997), we conclude that the Ca^{2+} transients were dependent primarily on Ca^{2+} entry through activated CNG channels.

Olfactory cilia function as individual biochemical compartments

To test more rigorously whether the signals indeed reflected ciliary odor detection, we applied spatially restricted odor pulses that contacted only a single cilium of a given neuron (Fig. 5). Only those cilia that were exposed to odor ligand responded with a fluoresence signal, whereas the remaining cilia showed no response (Fig. 5*A*). Subsequent stimulation of all cilia of a given cell demonstrated that all cilia had the ability to respond (Fig. 5*B*; $n = 4$ ORNs). Thus, the interaction of odor ligand with the presumed odor receptors can create highly localized odor-induced fluorescence signals in a single cilium. The signals originate in the cilia; there is no evidence for back spread of Ca^{2+} from the dendritic knob during the phase of initiation of the odor response. This supports the previous results (Fig. 3*B*), showing that each cilium can detect the presence of odor ligand and can function as a relatively independent Ca^{2+}-signaling unit.

That each of the cilia of a given ORN is responsive to odor stimuli was further shown by analyzing the Ca^{2+} transients from all cilia of an ORN caused by a single odor pulse (cineole, 300 μM) (Fig. 6*A*). More importantly, the kinetic features of the Ca^{2+} signals in all of the cilia on an individual ORN were surprisingly similar (Fig. 6*B*). Rescaling and superimposing eight individual odor-induced Ca^{2+} transients revealed that their dynamic characteristics, including delay, rise time, and decay time, were nearly indistinguishable (Fig. 6*C*). Qualitatively similar results were obtained in two other ORNs using much lower cineole concentrations (20 μM). These data demonstrate that individual cilia of a given ORN can produce remarkably synchronized Ca^{2+} transients with relatively uniform kinetic properties in response to odor ligand.

Mapping the molecular receptive range of individual olfactory cilia

To test whether the cilia of a given ORN are similar in their odor sensitivity and thus produce similar response profiles or whether they respond differentially to different odor ligands, we analyzed the Ca^{2+} transients in several cilia of a given ORN and compared their responses to six different odor ligands (acetophenone, *n*-amyl acetate, isoamyl acetate, cineole, citralva, and ethyl bu-

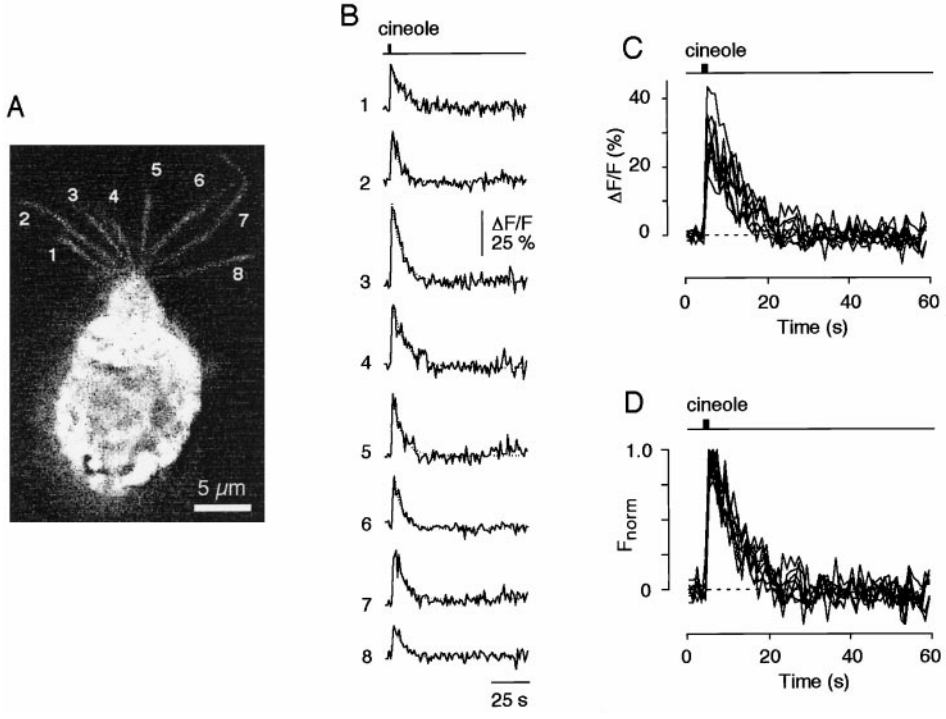

Figure 6. Individual cilia of a given ORN can produce synchronized Ca^{2+} transients with uniform kinetic properties after exposure to odor ligand. *A*, Fluorescence image (*gray scale*) of an ORN taken at peak fluorescence intensity after a 1 sec pulse of cineole (300 μM). Eight individual cilia (indicated by the numbers *1-8*) are clearly seen. *B*, Time course of the fluorescence response analyzed in all eight cilia. All cilia responded with a ciliary Ca^{2+} transient. *C, D*, Ca^{2+} responses were superimposed as original waveforms (*C*) or rescaled (*D*) to give the same peak amplitude. Note the remarkably similar time courses. Decay time constant, 7.7 ± 1.7 sec ($n = 8$).

tyrate; all at 300 μM). Figure 7 depicts the results from four single ORNs (cells *2*, *4*, *7*, and *10*; same neurons as listed in Fig. 2). In each of these cells three individual cilia were analyzed (cilia 1, 2, and 3). The data show that the response profiles tended to be very similar between individual cilia of a given cell, i.e., the overall tuning characteristics were preserved. However, the sensitivity to a given odor within the spectrum for a cell varied somewhat across different cilia. For example, in cell 2, the response amplitude for amyl acetate increases from cilium 1 to cilium 3, whereas the response amplitude for cineole decreases. For cell 7, a more complex relation is seen for the responses to three odors. Thus, there was uniformity for the odor selectivity of all cilia of a single cell, but there was a moderate degree of variability for the odor sensitivities of different cilia within the odor spectrum of that cell. The implications of these results will be discussed below.

Ciliary calcium transients are required for sensitivity regulation of odor transduction

What is the functional role of these localized odor-induced Ca^{2+} transients in olfactory signal transduction? Because changes in the intraciliary Ca^{2+} concentration are thought to mediate feedback regulation as part of odor adaptation in ORNs (Kurahashi and Shibuya, 1990; Zufall et al., 1991b; Jaworsky et al., 1995; Boekhoff et al., 1996; Kurahashi and Menini, 1997; Leinders-Zufall et al., 1997a), it is conceivable that the dynamics of Ca^{2+} changes determine the rate of these regulatory processes. To investigate this question, we compared the rate of recovery from odor adaptation with the rate of recovery of the Ca^{2+} transients. We measured recovery from adaptation by recording odor-induced membrane currents under voltage clamp using the perforated-patch technique (see Materials and Methods). ORNs were stimulated with identical odor pulses (300 μM cineole) using a paired-pulse paradigm (Fig. 8*A*). Consistent with previous reports (Kurahashi and Shibuya, 1990; Kurahashi and Menini, 1997), the peak amplitude of the response to the second pulse was small for short interpulse intervals (of a few seconds) but recovered as the interpulse interval increased (Fig. 8*A*). This short-term adaptation (STA) can be distinguished from a long-lasting form of odor adaptation (LLA) that can occur simultaneously in these neurons (Zufall and Leinders-Zufall, 1997; Ma et al., 1997). Figure 8*B* shows that the kinetics of Ca^{2+} recovery (continuous line, average from 23 cilia) were well correlated with the recovery from STA (single data points from eight ORNs), suggesting that odor adaptation might be controlled by the dynamics of odor-induced ciliary Ca^{2+} transients.

To demonstrate that Ca^{2+} increases are essential for odor adaptation, we tested the effect of BAPTA AM, a membrane-permeant intracellular Ca^{2+} chelator, on STA (Fig. 8*C*) ($n = 3$). Paired odor responses were elicited using an interpulse interval of 4 sec. Figure 8*C* shows that bath-applied BAPTA AM (100 μM) resulted in a nearly complete loss of STA. This was demonstrated by the time-dependent increase of the odor current caused by the second pulse, eventually reaching the same response magnitude as the first current. This effect of BAPTA AM occurred on a time scale that is consistent with the loading and cleavage of AMs in these neurons (Leinders-Zufall et al., 1997a). Together, these results indicate that odor-induced ciliary Ca^{2+} transients are essential for mediating negative feedback regulation of olfactory transduction.

DISCUSSION

A primary goal of this study was to develop an optical approach for real-time monitoring of odor responses at the sites of primary transduction in individual olfactory cilia. We show here that imaging odor-induced ciliary Ca^{2+} transients is an effective method for this purpose. The results are in general agreement with previous studies showing, with electrophysiological recordings, that the cilia are the sites of odor transduction (Firestein et al., 1990; Lowe and Gold, 1991, 1993a; see also Kleene et al., 1994 for a comprehensive survey of the electrical properties of olfactory cilia). They also support biochemical measurements on cell-

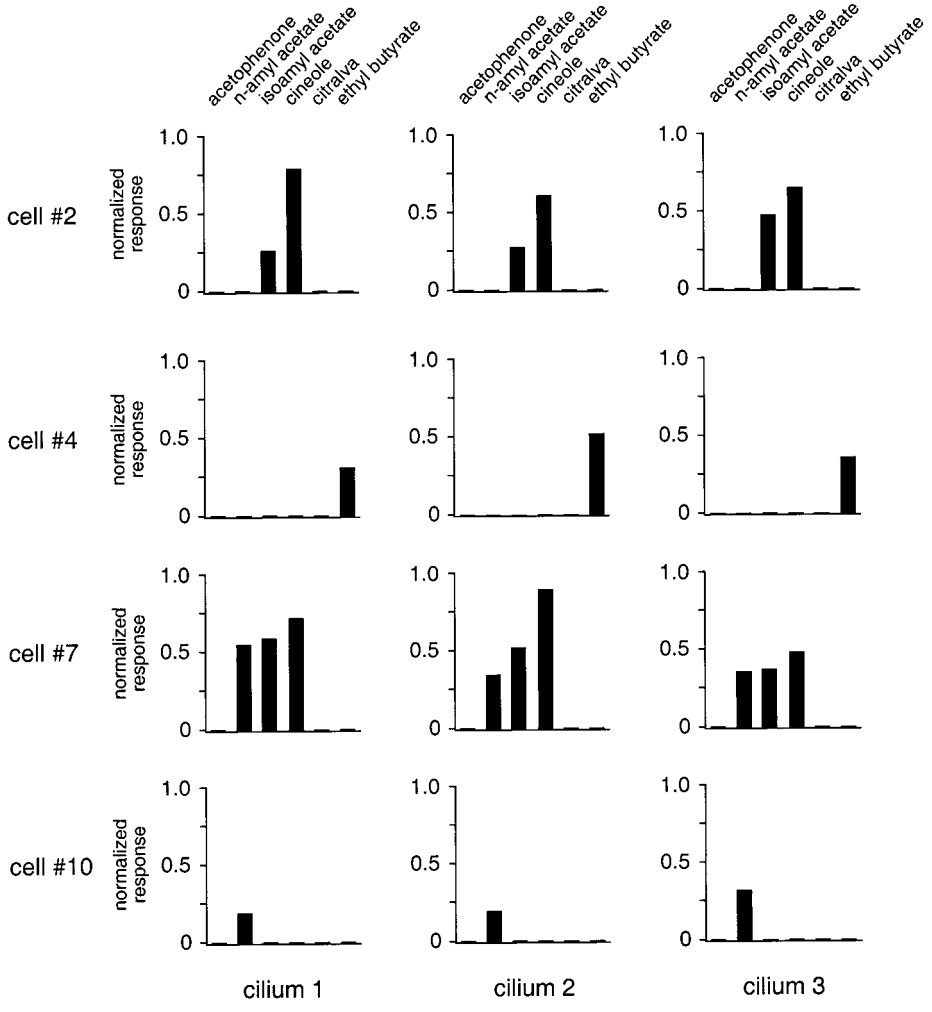

Figure 7. Plot of the response profiles of three individual cilia in four different ORNs (cells *2*, *4*, *7*, and *10*) in response to stimulation with the odor ligands acetophenone, *n*-amyl acetate, isoamyl acetate, cineole, citralva, and ethyl butyrate (all at 300 μM). Data are taken from the same pool of cells as shown in Figure 2, and the same analysis methods were applied to generate response profiles. Note that, in contrast to the discriminative variability seen between cells, there was only very little difference between the ciliary odor spectra for a single cell.

free cilia preparations demonstrating odor-dependent second messenger generation (Pace et al., 1985; Sklar et al., 1986; Breer et al., 1990). From these previous studies it was concluded that the entire primary transduction cascade necessary for the generation of odor-induced currents, from receptors to sensory membrane conductances, is present in the cilia. Our results confirm this conclusion and extend the analysis to direct recordings from the cilia themselves and to the level of individual cilia.

We have used laser scanning confocal microscopy of acutely isolated salamander ORNs that were firmly attached to the substrate, an approach that was introduced in our previous work (Leinders-Zufall et al., 1997a). This procedure takes advantage of the spatial resolution of the confocal microscope and the fact that, under our experimental conditions, all olfactory cilia are localized in the same focal plane. Immobilization of olfactory cilia allows also for micropulse stimulation of individual cilia under visual control and mapping of odor specificity within subcellular compartments. These specific conditions are necessary to ensure that the measured ciliary fluorescence changes are not attributable to movement artifacts or other changes such as shifts in pH or protein binding.

Properties of the odor-induced ciliary calcium transients

A number of studies in the salamander have established that the odor ligands used in this work evoke responses through activation of the cAMP second messenger system (cf. Zufall et al., 1994) but not through the IP_3 second messenger system (Firestein et al., 1991a; Lowe and Gold, 1993a); targeted disruption of the CNG channel α subunit abolished all odor responses in mouse olfactory epithelium (Brunet et al., 1996), and odor-induced Ca^{2+} changes within the cilia can be mimicked by application of the phosphodiesterase inhibitor IBMX (Leinders-Zufall et al., 1997a), which is known to increase activation of CNG channels (Firestein et al., 1991b; Lowe and Gold 1993b). These studies together with the results summarized here analyzing the kinetic and pharmacological properties of ciliary Ca^{2+} transients as well as their distinct odor specificity and dependence on odor concentration support the notion that the ciliary Ca^{2+} signals observed in this study resulted from Ca^{2+} entry through CNG channels after activation of the odor-stimulated cAMP pathway of these neurons.

The basic properties of the ciliary Ca^{2+} transients may be summarized as follows. In response to an odor pulse, the transients rise rapidly within 1 sec and decay with a time constant of ~5 sec (at odor concentrations used here). The ciliary Ca^{2+} transients precede the transients observed in the knob, dendrite, and soma. The cilia of a given ORN are also relatively uniform in their response kinetics, i.e., the rise time and decay from the peak of the response. The ciliary transients show selective responses to different odor stimuli, similar to the selective responses of sensory membrane currents seen in whole-cell recordings from

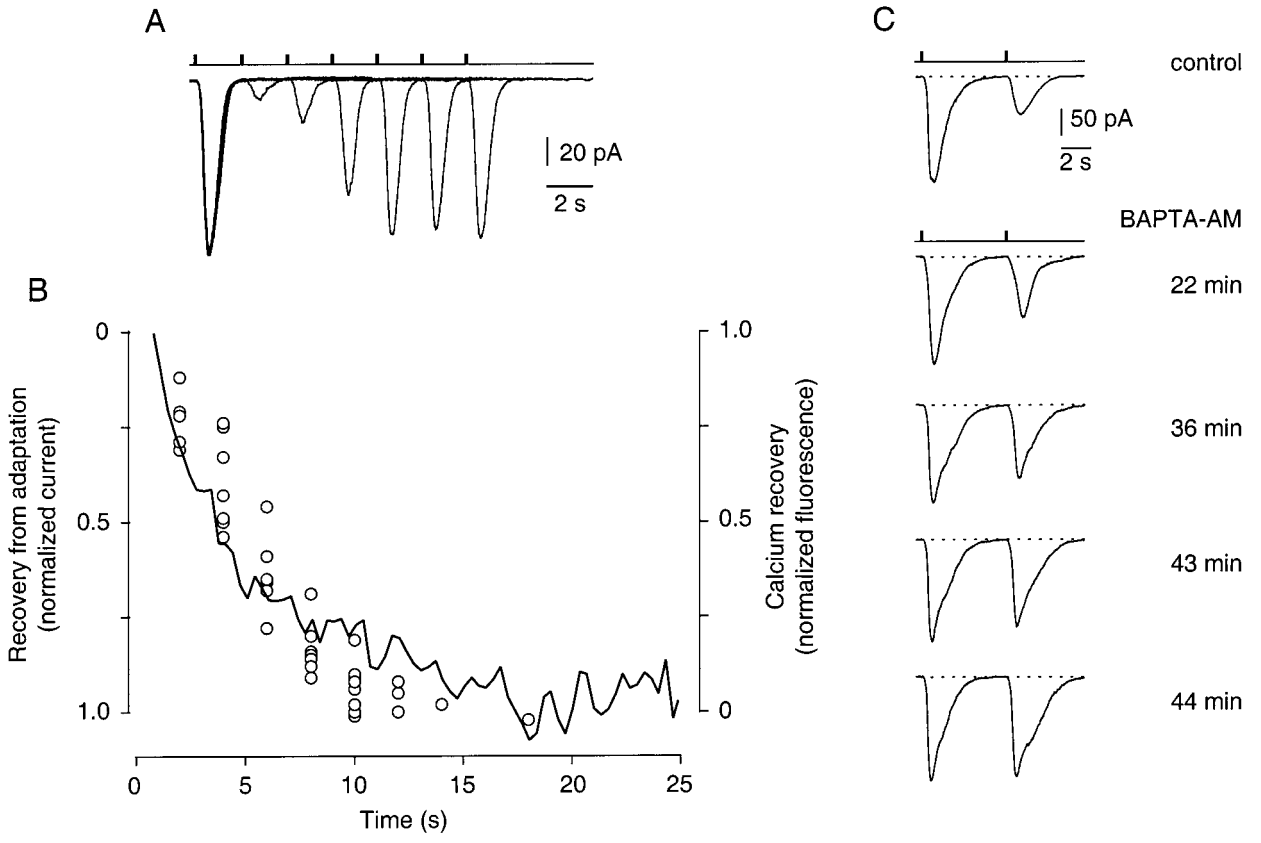

Figure 8. Evidence that Ca^{2+} transients are required for odor adaptation. *A*, An ORN was stimulated with identical paired pulses of cineole (300 μM) that were delivered every 40 sec. The cell was voltage clamped to −60 mV, and the resulting membrane currents were monitored and superimposed. For an interpulse interval of 2 sec between the first and second stimulus, the second pulse elicited a strongly declined peak response. Recovery from this reduced responsiveness was monitored by increasing the interpulse interval. *B*, The recovery from short-term odor adaptation matches the recovery time course of the ciliary Ca^{2+} transients. Shown are normalized, averaged Ca^{2+} responses (cineole, 300 μM) from five ORNs (23 cilia) (*solid line*). The decay time course was fitted with a single exponential function giving a time constant $\tau = 5.1$ sec. Superimposed in this graph is the recovery from odor adaptation measured in eight individual ORNs (*open circles*) using the protocol shown in *A*. The responses are expressed as a percentage of the fully recovered amplitude. Employing a nonlinear least squares fitting routine, the data points were fitted with a single exponential function of a time constant $\tau = 5.6$ sec (data not shown). *C*, Short-term adaptation is disrupted after bath-application of the membrane-permeant intracellular Ca^{2+} chelator BAPTA AM (100 μM). Paired odor responses (cineole, 300 μM) are elicited at fixed interval of 4 sec. As the BAPTA AM is taken up by the cell and cleaved by endogenous esterases the response to the second pulse becomes larger until it eventually matches the first response.

salamander ORNs (Firestein et al., 1993). The cilia of a given ORN are relatively uniform in their responses to different odors; in other words, they have similar molecular receptive ranges or odor sensitivity spectra. However, the relative response magnitudes of individual cilia to a given single odor stimulus can vary.

The Ca^{2+} signals recorded in a cilium during an odor response showed notable variations in distribution of fluorescence intensity at the single-pixel level along the length of the cilium. One possibility is that these highly localized regions of fluorescence elevation (hot spots) reflected the fact that the signals were caused by inhomogeneous dye distribution. Alternatively, this result could reflect the clustering of odor receptors or of other elements of the second messenger cascades, e.g., CNG channels or Ca^{2+} extrusion sites (for a discussion of the ultrastructural aspects of ciliary signaling; see Menco, 1997). Future improvement of the imaging technology should enable us to distinguish between these possibilities.

Possible significance of variations in cilia responsiveness

As noted above, when a cell was selectively responsive to an odor stimulus, all of the cilia showed the same selectivity. This responsiveness was relatively uniform between different cilia, but there were small differences in amplitude that may be significant. Thus, as shown in Figure 7, when a cell was responsive to both isoamyl acetate and cineole (e.g., cells 2 and 7), all three of the cilia measured showed responses to both odors. However, between cilia the magnitudes of the responses showed small variations, and of particular interest, these amplitudes could vary in opposite directions. Thus, for cell 7 the response to amyl acetate was smaller in cilium 2 compared with cilium 1, whereas the response to cineole was larger in cilium 2 compared with cilium 1.

There are several possibilities that could account for this finding. First, it could be attributable to variations in the diameters of these cilia, but it would be difficult to account for the opposite variations for two different odors on this basis. Second, it could be attributable to receptors with differing affinities for these two odors, either sequence variations within one receptor type or two different receptors. Third, there could be differences in the second messenger regulation within different cilia. Fourth, there could be differences in accessing of the different cilia by the different odors. Fifth, they could reflect limitations in the sensitivity of the imaging method for the different odors. Sixth, they

could reflect a degree of variability of repeated responses from the same cilium. Given that the array of cilia extending from a single ORN is likely to provide a mechanism for the spatial summation of electrical signals generated at distinct ciliary sites of an ORN, it remains to be seen whether these small differences in Ca^{2+} responsiveness between the cilia of a single cell indeed reflect physiological properties of the signaling pathway.

Role of ciliary calcium transients in sensory adaptation

A finding of importance is that the dynamics of odor-induced Ca^{2+} changes in the olfactory cilia appear to determine the rate of odor adaptation (Fig. 8). The kinetics of recovery of the Ca^{2+} transients identified here closely match the recovery from a short-term form of odor adaptation as seen by using a paired-pulse paradigm of odor stimulation. Treatment of the ORNs with the membrane-permeant Ca^{2+} chelator BAPTA AM eliminates this odor adaptation. Both of these results imply that the ciliary Ca^{2+} transients are required for sensitivity regulation of odor transduction under conditions of repetitive stimulation. Interestingly, this critical role of Ca^{2+} entry through transduction channels for adaptation of olfactory neurons bears striking resemblance to adaptation processes in other sensory neurons such as vertebrate and invertebrate photoreceptor cells (cf. Ranganathan et al., 1994; Koutalos and Yau, 1996) and mechanosensory hair cells (Denk et al., 1995; Walker and Hudspeth, 1996, and references therein). Using calibration methods reported previously (Leinders-Zufall et al., 1997a) we approximately estimate a low resting Ca^{2+} level in olfactory cilia of ~40 nM. The relative fluorescence changes ($\Delta F/F$) of ~6.0–51% in the cilia caused by odor pulses then correspond to a change in $[Ca^{2+}]_i$ of ~20–300 nM. These rises would not be sufficient for downregulating CNG channel activity through Ca^{2+}-calmodulin, which has been proposed as the main mechanism underlying odor adaptation (Chen and Yau, 1994; Kurahashi and Menini, 1997). They would, however, be adequate to downregulate odor-stimulated adenylyl cyclase activity (Boekhoff et al., 1996). It seems likely that ultramicro domains of much higher Ca^{2+} levels exist in close proximity to each conducting CNG channel, as has been postulated in a number of other signaling processes (for review, see Neher, 1998). Future use of so-called near-membrane Ca^{2+} indicators that monitor Ca^{2+} changes primarily associated with the plasma membrane (cf. Etter et al., 1996) may allow resolution of this issue.

Conclusion

Imaging odor-induced Ca^{2+} changes has enabled us to monitor, in a spatially resolved manner and at anatomically distinct sites, the initial steps leading to olfactory perception. The present results establish the olfactory receptor cell cilia as fundamental functional compartments that control both selectivity and response magnitude of the olfactory system. The ability to visualize molecular events associated with odor detection at the level of single cilia may allow future studies to be directed toward elucidating the dynamics of the receptor site and monitoring single interactions of odor ligand with olfactory receptors through optical quantal analysis.

REFERENCES

Belluscio L, Gold GH, Nemes A, Axel R (1998) Mice deficient in G_{olf} are anosmic. Neuron 20:69–81.

Boekhoff I, Kroner C, Breer H (1996) Calcium controls second-messenger signalling in olfactory cilia. Cell Signal 8:167–171.

Bozza TC, Kauer JS (1997) Odorant response properties of convergent olfactory receptor neurons in the mouse olfactory system. Soc Neurosci Abstr 23:741.

Breer H, Boekhoff I, Tareilus E (1990) Rapid kinetics of second messenger formation in olfactory transduction. Nature 345:65–68.

Brunet LJ, Gold GH, Ngai J (1996) General anosmia caused by a targeted disruption of the mouse olfactory cyclic nucleotide-gated cation channel. Neuron 17:681–693.

Buck L, Axel R (1991) A novel multigene family may encode odorant receptors: a molecular basis for odor recognition. Cell 65:175–187.

Chen T-Y, Yau K-W (1994) Direct modulation by Ca^{2+}-calmodulin of cyclic nucleotide-activated channel of rat olfactory receptor neurons. Nature 368:545–548.

Denk W, Holt JR, Shepherd GMG, Corey DP (1995) Calcium imaging of single stereocilia in hair cells: Localization of transduction channels at both ends of tip links. Neuron 15:1311–1321.

Dhallan RS, Yau K-W, Schrader KA, Reed RR (1990) Primary structure and functional expression of a cyclic nucleotide-gated channel from olfactory neurons. Nature 347:184–187.

Etter EF, Minta A, Poenie M, Fay FS (1996) Near-membrane $[Ca^{2+}]$ transients resolved using the Ca^{2+} indicator FFP18. Proc Natl Acad Sci USA 28:5368–5373.

Firestein S, Shepherd GM, Werblin FS (1990) Time course of the membrane current underlying sensory transduction in salamander olfactory receptor neurones. J Physiol (Lond) 430:135–158.

Firestein S, Darrow B, Shepherd GM (1991a) Activation of the sensory current in salamander olfactory receptor neurons depends on a G-protein mediated cAMP second messenger system. Neuron 6:825–835.

Firestein S, Zufall F, Shepherd GM (1991b) Single odor-sensitive channels in olfactory receptor neurons are also gated by cyclic nucleotides. J Neurosci 11:3565–3572.

Firestein S, Picco C, Menini A (1993) The relation between stimulus and response in olfactory receptor cells of the tiger salamander. J Physiol (Lond) 468:1–10.

Frings S, Seifert R, Godde M, Kaupp UB (1995) Profoundly different calcium permeation and blockage determine the specific function of distinct cyclic nucleotide-gated channels. Neuron 15:169–179.

Jaworsky DE, Matsuzaki O, Borisy FF, Ronnett GV (1995) Calcium modulates the rapid kinetics of the odorant-induced cyclic AMP signal in rat olfactory cilia. J Neurosci 15:310–318.

Kao JPY, Harootunian AT, Tsien RY (1989) Photochemically generated cytosolic calcium pulses and their detection by fluo-3. J Biol Chem 264:8179–8

Kleene SJ, Gesteland RC, Bryant SH (1994) An electrophysiological survey of frog olfactory cilia. J Exp Biol 195:307–328.

Koutalos Y, Yau K-W (1996) Regulation of sensitivity in vertebrate rod photoreceptors by calcium. Trends Neurosci 19:73–81.

Kurahashi T (1990) The response induced by intracellular cyclic AMP in isolated olfactory receptor cells of the newt. J Physiol (Lond) 430:355–371.

Kurahashi T, Shibuya T (1990) Ca^{2+}-dependent adaptive properties in the solitary olfactory receptor cells of the newt. Brain Res 515:261–268.

Kurahashi T, Menini A (1997) Mechanism of odorant adaptation in the olfactory receptor cell. Nature 385:725–729.

Leinders-Zufall T, Zufall F (1995) Block of cyclic nucleotide-gated channels in salamander olfactory receptor neurons by the guanylyl cyclase inhibitor LY83583. J Neurophysiol 74:2759–2762.

Leinders-Zufall T, Shepherd GM, Zufall F (1995) Regulation of cyclic nucleotide-gated channels and membrane excitability in olfactory receptor cells by carbon monoxide. J Neurophysiol 74:1498–1508.

Leinders-Zufall T, Shepherd GM, Zufall F (1996) Modulation by cyclic GMP of the odor sensitivity of vertebrate olfactory receptor cells. Proc R Soc Lond B Biol Sci 263:803–811.

Leinders-Zufall T, Rand MN, Shepherd GM, Greer CA, Zufall F (1997a) Calcium entry through cyclic nucleotide-gated channels in individual cilia of olfactory receptor cells: spatiotemporal dynamics. J Neurosci 17:4136–4148.

Leinders-Zufall T, Rand MN, Shepherd GM, Greer CA, Zufall F (1997b) Visualizing odor detection in single olfactory cilia by monitoring calcium entry through cyclic nucleotide-gated channels. Biophys J 72:A286.

Lischka FW, Schild D (1993) Standing calcium gradients in olfactory receptor neurons can be abolished by amiloride or ruthenium red. J Gen Physiol 102:817–831.

Lowe G, Gold GH (1991) The spatial distributions of odorant sensitivity and odorant-induced currents in salamander olfactory receptor cells. J Physiol (Lond) 442:147–168.

Lowe G, Gold GH (1993a) Contribution of the ciliary cyclic nucleotide-gated conductance to olfactory transduction in the salamander. J Physiol (Lond) 462:175–196.

Lowe G, Gold GH (1993b) Nonlinear amplification by calcium-dependent chloride channels in olfactory receptor cells. Nature 366:283–286.

Lumpkin EA, Hudspeth AJ (1995) Detection of Ca^{2+} entry through mechanosensitive channels localizes the site of mechanoelectrical transduction in hair cells. Proc Natl Acad Sci USA 92:10297–10301.

Ma M, Leinders-Zufall T, Shepherd GM, Zufall F (1997) Two forms of odor adaptation in single olfactory receptor neurons. Soc Neurosci Abstr 23:741.

Menco BPM (1997) Ultrastructural aspects of olfactory signaling. Chem Senses 22:295–311.

Morales B, Madrid R, Bacigalupo J (1997) Calcium mediates the activation of the inhibitory current induced by odorants in toad olfactory receptor neurons. FEBS Lett 402:259–264.

Nakamura T, Gold GH (1987) A cyclic-nucleotide gated conductance in olfactory receptor cilia. Nature 325:442–444.

Nakamura T, Tsuru K, Miyamoto S (1994) Regulation of Ca^{2+} concentration by second messengers in newt olfactory receptor cell. Neurosci Lett 171:197–200.

Neher E (1998) Vesicle pools and Ca^{2+} microdomains: new tools for understanding their roles in neurotransmitter release. Neuron 20:389–399.

Pace U, Hanski E, Salomon Y, Lancet D (1985) Odorant-sensitive adenylate cyclase may mediate olfactory reception. Nature 316: 255–258.

Ranganathan R, Bacskai BJ, Tsien RY, Zuker CS (1994) Cytosolic calcium transients: spatial localization and role in *Drosophila* photoreceptor cell function. Neuron 13:837–848.

Reed RR (1992) Signaling pathways in odorant detection. Neuron 8:205–209.

Restrepo D, Okada Y, Teeter JH (1993) Odorant-regulated Ca^{2+} gradients in rat olfactory neurons. J Gen Physiol 102:907–924.

Sato T, Hirono J, Tonoike M, Takebayshi M (1994) Tuning specificities to aliphatic odorants in mouse olfactory receptor neurons and their local distribution. J Neurophysiol 72:2980–2989.

Sklar PB, Anholt RRH, Snyder SH (1986) The odorant-sensitive adenylate cyclase of olfactory receptor cells. J Biol Chem 261: 15538–15543.

Tareilus E, Noé J, Breer H (1995) Calcium signals in olfactory neurons. Biochim Biophys Acta 1269:129–138.

Walker RG, Hudspeth AJ (1996) Calmodulin controls adaptation of mechanoelectrical transduction by hair cells of the bullfrog's sacculus. Proc Natl Acad Sci USA 93:2203–2207.

Zagotta WN, Siegelbaum SA (1996) Structure and function of cyclic nucleotide-gated channels. Annu Rev Neurosci 19:235–263.

Zhao H, Ivic L, Otaki JM, Hashimoto M, Mikoshiba K, Firestein S (1998) Functional expression of a mammalian odorant receptor. Science 279:237–242.

Zufall F, Firestein S, Shepherd GM (1991a) Analysis of single cyclic nucleotide gated channels in olfactory receptor cells. J Neurosci 11:3573–3580.

Zufall F, Shepherd GM, Firestein S (1991b) Inhibition of the olfactory cyclic nucleotide gated ion channel by intracellular calcium. Proc R Soc Lond B Biol Sci 246:225–230.

Zufall F, Firestein S, Shepherd GM (1994) Cyclic nucleotide gated channels and sensory transduction in olfactory receptor neurons. Annu Rev Biophys Biomol Struct 23:577–607.

Zufall F, Leinders-Zufall T (1997) Identification of a long-lasting form of odor adaptation that depends on the carbon monoxide/cGMP second messenger system. J Neurosci 17:2703–2712.

Zufall F, Leinders-Zufall T, Shepherd GM, Greer, CA (1997) Calcium store depletion by thapsigargin does not affect olfactory signal transduction. Soc Neurosci Abstr 23:741.